Lengthening Kinetics of Ferrite and Bainite Sideplate

E. P. SIMONEN, H. I. AARONSON, AND R. TRIVEDI

The rate of lengthening of ferrite and bainite sideplates and the radius of curvature of the plate edges were measured as a function of reaction temperature in three Fe-C alloys. These data were analyzed on the basis of an equation due to Trivedi. The analysis proved that the mobility of the sideplate edges is limited. The interfacial energy of these edges is of the order of 200 erg/cm^2. Most of the supersaturation is used to drive the diffusion of carbon in austenite; comparatively little is accounted for by capillarity and by the finite mobility of the interface. On the basis of both the present results and of published microstructural observations, it was concluded that ferrite and bainite sideplates lengthen by a ledge mechanism.

ACCORDING to the initial form of a general theory of precipitate morphology,[1] plate-shaped precipitates develop because there is a barrier to growth only in the direction normal to their broad faces. The barrier takes the form of a partially or fully coherent interfacial structure; this structure can be displaced only by the operation of a ledge mechanism, and the overall kinetics of displacement in the direction normal to the boundary are less than those allowed by long-range volume diffusion control. At all other orientations of the boundary, a disordered or incoherent interfacial structure, which normally does not interfere with growth, was proposed. Such a structure ought thus to obtain at the edges of precipitate plates. Both the structural and the kinetic predictions which this theory makes with respect to the broad faces of plates have been experimentally validated in three nonferrous alloy systems.[2-6] Also, proeutectoid ferrite plates formed in Fe-C alloys have been recently shown to thicken by the ledge mechanism.[7] By analogy to recent observations and deductions on the structurally similar formation of chromium-rich precipitates in a Cu-Cr alloy,[8] the broad faces of ferrite plates can probably be safely considered as partially coherent.

The view that the edges of precipitate plates have a disordered structure, however, has not fared as well. Needles of α Cu-Zn do appear to lengthen with volume diffusion controlled kinetics,[9] suggesting that their tips have a disordered structure. On the other hand, the edges of θ' plates in Al-Cu[2] and the edges of γ plates in Al-Ag[4] have misfit dislocation structures. The former plates lengthen more rapidly than volume diffusion control allows; this was deduced to result from ledgewise lengthening accelerated by rapid diffusion along the misfit dislocations girdling the θ' plates.[3] Although γ plates in Al-Ag lengthen at overall rates approximately equal to those of volume diffusion control, visual observations made at the aging temperature proved that these plates also lengthen by a ledge mechanism.[5] The theory of morphology has accordingly been revised to state that even when there is a growth barrier at more than one boundary orientation, plates can still form as long as the ledges are either much more widely spaced or migrate much more slowly at one such orientation.[10]

In the case of proeutectoid ferrite plates, the evidence on the mechanism of lengthening is conflicting. On one hand, Eichen *et al.*[11] found a rather coarse le structure at the edges of ferrite plates by optical mi croscopy and the method of multiple sectioning, and Davenport[12] recently observed finer scale ledges whe examining plate edges by transmission electron microscopy. On the other hand, agreement between the theoretical treatment of plate lengthening by Kaufma Radcliffe and Cohen (KRC),[13] performed on the assun tion that lengthening is controlled by the volume diffu sion of carbon in austenite, and the kinetic data (on F C alloys) of Hillert[14] and Speich and Cohen[15] is improved if the edges of ferrite plates are assigned an interfacial energy appropriate to a disordered auster ite:ferrite boundary.[16] The calculations of ferrite pl lengthening kinetics reported by Paxton and Pound[16] yield a similar result. Recently, however, a theoreti cal treatment of plate lengthening which is both mor rigorous and more general has become available.[17] The present study was undertaken to reexamine the lengthening mechanism of ferrite plates upon the ba of this treatment. The experimental data required ir clude not only rates of lengthening but also the radiu of curvature of plate edges. Although a considerable amount of data on the lengthening rate of ferrite plat and bainite in Fe-C alloys is now available,[1,14,15,18] very few measurements of the radius of curvature o ferrite plate edges have been reported.[1] Since it appears important that both types of data be taken fron the same alloys in view of the possible effects of im purities upon the radius of curvature, these two mea surements were made together as a function of reac tion temperature on a series of Fe-C alloys. It will be seen that the combination of the rigorous theoreti cal treatment and the new experimental data leads tc a conclusion as to the mechanism of ferrite plate lengthening quite different from that reached on the basis of previous kinetic studies, but in good accord with the microstructural observations.

EXPERIMENTAL PROCEDURE

The alloys used in this investigation were prepare by vacuum melting and casting. Their compositions are given in Table I. Specimens 6 by 6 by 0.8 mm machined from these alloys were austenitized for 30 min at 1300°C in a graphite-deoxidized, argon-pro-

E. P. SIMONEN is with Battelle Northwest, Richland, Wash. 99352. H. I. AARONSON is Professor, Michigan Technological University, Houghton, Mich. 49931. R. TRIVEDI is Associate Professor, Institute for Atomic Research and Department of Metallurgy, Iowa State University, Ames, Iowa 50010.

Manuscript submitted July 24, 1972.

Table I. Designation and Composition of Alloys Used for Kinetic and Radii Measurements

Designation	Composition of Alloys				
	Pct C	Pct Si	Pct Mn	Pct P	Pct S
I	0.24	0.003	0.002	0.001	0.005
II	0.33	0.002	0.002	0.001	0.005
III	0.43	0.004	0.002	0.001	0.004

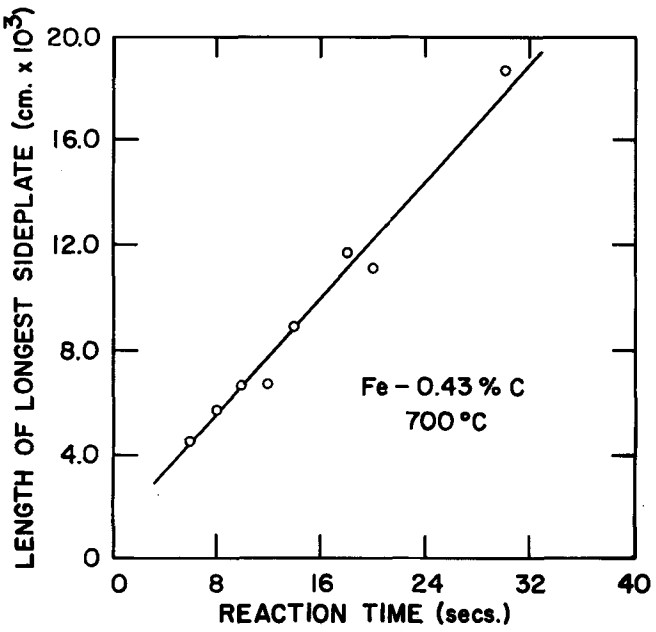

Fig. 1—Length of longest sideplate vs. reaction time for isothermal treatment of the 0.24 pct C alloy at 700°C.

tected bath of molten $BaCl_2$,[19] isothermally reacted in deoxidized lead baths and rapidly quenched into iced 10 pct brine. Isothermal reaction temperatures ranged from 450° to 700°C.

Rates of lengthening were measured on sideplates, by determining the length of the longest sideplate on the plane of polish as a function of isothermal reaction time. Since these rates were constant, in agreement with the results of previous investigators,[1,14,15,18] it was necessary to measure the radius of curvature of plate edges at only one reaction time at a given temperature. The smallness of the radii necessitated the use of replication electron microscopy. Carbon replicas, shadowed with platinum, were employed; the amount of shadowing was held to the minimum level needed to obtain sharp images of the tips. Radii were measured from electron micrographs taken at 20,000 to 30,000 diam. At each alloy composition and reaction temperature employed, a frequency histogram was constructed from 50 to 100 measurements. The radii of curvature used in the comparisons between theory and experiment were those corresponding to the maxima in the histograms.

RESULTS

Fig. 1 shows a typical plot of maximum sideplate length vs. isothermal reaction time. The slope of this plot gives the rate of lengthening. Table II summarizes the results obtained for the growth rate as a function of reaction temperature and alloy composition. Some of Hillert's[14] data on Fe-C alloys have also been included in this table. Since the lengthening rate at a given temperature should decrease with increasing carbon content of the alloy, the two sets of data are seen to be at least qualitatively consistent at 700°C, but to diverge somewhat, though not very badly, at 650°C. Comparable levels of agreement were achieved with the results of Townsend and Kirkaldy.[18]

Table II. Experimental Lengthening Rate of Widmanstatten Precipitates as a Function of Temperature and Composition. The Measurements in the 0.29 Pct C and 0.49 Pct C Alloys are Those of Hillert.[14]

T°C	Lengthening Rate cm/s X 10^{-3}				
	0.24 Pct C	0.29 Pct C	0.33 Pct C	0.43 Pct C	0.49 Pct C
700	2.1	1.6*	1.3	0.6	0.2*
650	2.2	2.2*	1.5	0.8	1.0*
550	2.5		2.2	1.3	
450	3.2		2.3		

*Hillert.

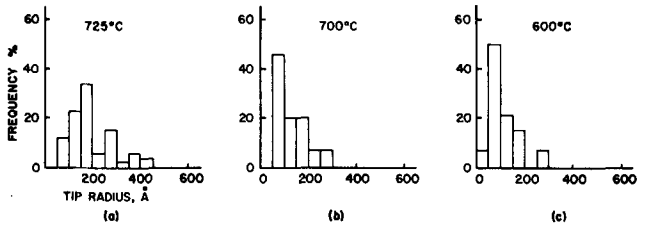

Fig. 2—Frequency histograms of the radii of curvature data in the 0.24 pct C alloy at the indicated reaction temperature.

Fig. 2 shows typical frequency histograms of the radius of curvature data, for three different reaction temperatures in the 0.24 pct C alloy. Smooth curves drawn through these sets of data are superimposed in Fig. 3. As the temperature decreases, the histograms become narrower. Yost and Trivedi[20] have shown that this result is consistent with determination of the rate of lengthening by the maximum growth rate principle. The maxima of the histograms are listed in Table III.

DISCUSSION

Theoretical Model

Several of the major theoretical models for the kinetics of lengthening of plates,[21-23] all developed under the assumption that the rate-limiting factor is long-range volume diffusion, have been critically reviewed by Trivedi and Pound.[24] A treatment recently developed by Trivedi[17] also takes account of the effects upon lengthening kinetics of the interfacial mobility of the plate edges. This is expressed as an interface kinetic coefficient, μ_0. (This coefficient will later be considered qualitatively in terms of the ledge mechanism.) Trivedi's result, which implicitly relates the lengthening rate, V, to μ_0, the radius of curvature of the plate edges, ρ, and the normalized supersaturation, Ω_0, is:

$$\Omega_0 = \sqrt{\pi p}\, e^p\, erfc(\sqrt{p})\left[1 + \frac{V}{V_c}\,\Omega_0 S_1\{p\} + \frac{\rho_c}{\rho}\,\Omega_0 S_2\{p\}\right] \quad [1]$$

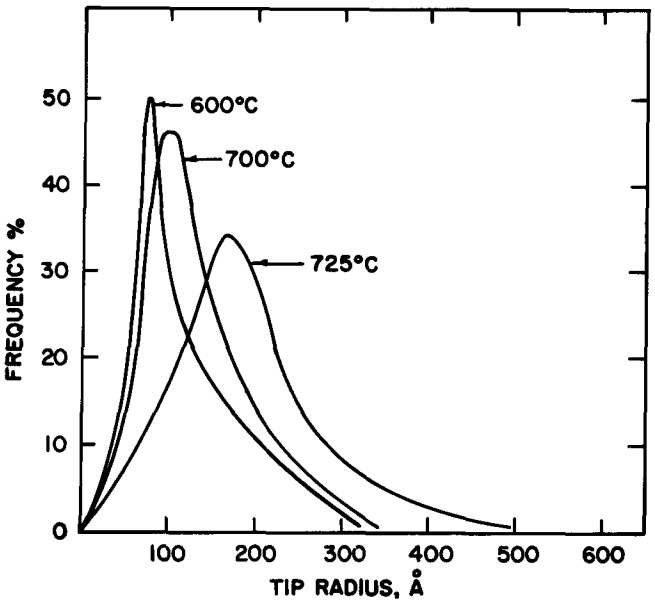

Fig. 3—Smooth curves drawn through the histograms shown in Fig. 2. The three curves are superimposed to illustrate the effect of temperature on the histogram shape.

Table III. Experimental Radii of Curvature as a Function of Temperature and Composition

	Radius of Curvature Data		
	ρÅ		
T, °C	0.24 Pct C	0.33 Pct C	0.43 Pct C
750	180		
725	165	230	
700	95	155	180
600	75		
550	65	120	70
500	60		
360	65		

where $\Omega_0 = (C_0 - C_\infty)/(C_0 - C_p)$, C_0 and C_p = mole fractions of solute at planar, disordered boundaries in the matrix and in the precipitate, respectively, at the matrix:precipitate boundary, and C_∞ = mole fraction of solute in the alloy. p = a dimensionless parameter equal to $V\rho/2D$, where D = an appropriate diffusion coefficient (in the present situation, the diffusivity of carbon in austenite). ρ_c = equilibrium critical radius, equal to $(C_0\Gamma)/(C_0 - C_\infty)$; Γ will be defined later, in connection with Eq. [4*b*]. V_c, the critical velocity, is that which would result if the interface were flat and its velocity were controlled entirely by the kinetics of interfacial reaction:

$$V_c = \mu_0(C_0 - C_\infty) \qquad [2]$$

$S_1\{p\}$ and $S_2\{p\}$ are complicated functions of p and are defined in Ref. 17.

The normalized supersaturation is essentially divided into three additive terms in Eq. [1]. These terms represent the fraction of Ω_0 consumed by diffusion, interface resistance and capillarity processes, respectively. Note that Eq. [1] gives the relationship between V and ρ for a given value of Ω_0. The optimization principle of maximum growth rate[21] is used to obtain uniquely the values of V and ρ.

Before applying Eq. [1] to the experimental data it will be necessary to examine critically some of the parameters and assumptions involved in the theoretical model.

1) In the derivation of Eq. [1], the diffusion coefficient is assumed to be independent of concentration, however, the diffusivity of carbon in austenite varies exponentially with carbon concentration.[25] This variation becomes important at lower transformation temperatures where the concentration difference $(C_t - C_\infty)$, C_t being the actual solute concentration at the tip of the plate, becomes quite large. As shown by Trivedi and Pound,[26] the concentration-dependence of the diffusion coefficient can be taken into account by using an average diffusion coefficient defined as

$$D_{ave} = \frac{1}{(C_t - C_\infty)} \int_{C_\infty}^{C_t} D\,dc \qquad [3]$$

This value will be used in subsequent calculations utilizing the diffusivity data of Wells, Batz, and Mehl.[25]

2) The theoretical result requires knowledge of C_0 and C_p. Their values are well established above the eutectoid temperature. However, the experimental data are at lower temperatures where extrapolation of the phase boundaries is required. Various models are available for such an extrapolation,[13,28] which give almost the same result near (and above) the eutectoid temperature but differ considerably at temperatures appreciably below. According to Ban-ya, Elliot, and Chipmann[27] the Lacher-Fowler-Guggenheim equation used by Aaronson, Domian, and Pound (ADP)[28] is a good one. Therefore, the ADP results were utilized to extrapolate the phase boundaries below the eutectoid temperature.

3) Eq. [1] is based on a linear relationship between the equilibrium concentration and the curvature of the interface. The linear relationship employed, however, is not the one appropriate for dilute solutions. Detailed numerical calculations[26] of the equilibrium concentration, C_ρ, as a function of interface curvature, ρ, show that considerable departure from linearity occurs when the radius of curvature is varied from ρ_c to infinity. Theoretical calculations on the radius of curvature corresponding to the maximum growth rate—which is the measurement resulting from the experimental technique employed—indicate, however, that this radius is always equal to or greater than twice the critical radius. And it turns out that in the region $2\rho_c \leq \rho < \infty$ the following linear expression for the equilibrium concentration fits quite accurately the numerical calculations of Trivedi and Pound:[26]

$$C_\rho = C_0 - C_0\Gamma K, \qquad [4a]$$

$$\Gamma = \frac{\sigma \bar{V}^{\alpha}_{Fe}}{RT}\left(-\frac{RT}{\Delta G^{\gamma\rightarrow\alpha}_{Fe}} - b\right), \qquad [4b]$$

and

$$b = -1.19778\times10^{-5}(T - 852.0)^2 + 1.699733. \qquad [4c]$$

where σ, $\bar{V}^{\alpha}_{Fe}$, and R are interfacial free energy, partial molar volume of iron in the precipitate and the gas constant, respectively, and $K = \rho^{-1}\cdot\Delta G^{\gamma\rightarrow\alpha}_{Fe}$ is the free energy change per mole for the $\gamma \rightarrow \alpha$ transformation in pure iron. The above result is valid for the temperature range 450° to 750°C and is accurate to

within three percent of the rigorous numerical calculations. Note that when b is neglected the present capillarity predictions are identical with those of Paxton and Pound.[16]

4) A knowledge of the interfacial energy, σ, and the interface kinetic coefficient, μ_0, is required. In the present work, however, these parameters are deduced by fitting the theory to the experimental values of growth rate and radius of curvature. The values obtained are considered in the final section of the paper.

5) Eq. [1] is derived on the assumption that free energy dissipation due to the motion of the interface results in a deviation in the carbon concentration in austenite at the interface from C_ρ. The velocity of the interface is then assumed to be linearly proportional to this deviation, *i.e.*,

$$V = \mu_0 \Delta C_k \qquad [5]$$

where

$$\Delta C_k = C_\rho - C_t.$$

Analysis of Experimental Results

Eqs. [1] to [4] can now be used to calculate the growth rate and radius of curvature at the plate tip as a function of supersaturation. We shall first assume that the mobility of the interface is infinite so that driving force required for the interface motion is negligible. Figs. 4(*a*) and 4(*b*) compare the experimental results with the predicted growth rates calculated by using two values of interfacial free energy, viz., 200 erg/cm^2 and 800 erg/cm^2, the values which approximately correspond to partially coherent[13] and disordered[29] interfaces, respectively. The calculated growth rates in Fig. 4(*a*) (σ = 200 erg/cm^2) show excellent agreement with experiment at 700°C but predict much higher values at low temperatures; at 450°C the discrepancy amounts to an order of magnitude. Fig. 4(*b*) shows that the theoretical growth rates based on the assumption of disordered plate edges are smaller than the measured values at high temperatures but are again much larger at 450°C. In fact the highly implausible value of σ = 1400 erg/cm^2 is required to match the theoretical results with experiment at 450°C. These results clearly show that no interfacial energy value exists which will adequately describe the kinetic behavior over the entire temperature range if the plate edges are assumed to be infinitely mobile. In the present context, it only remains to note that on the basis of the previously mentioned theoretical result[17] that $\rho_c \leq \frac{1}{2}\rho$ (experimental). The measured data on radii can be shown to place an upper limit on σ of *ca.* 650 erg/cm^2, and thus fairly definitely exclude the possibility of entirely disordered plate edges.

We shall now calculate growth rates on the basis of a finite mobility of the interface. However, for these calculations, a value of interfacial energy must be estimated. If the interface has a finite mobility, the growth rates will be smaller than those calculated on the basis of local equilibrium at the interface. As shown in Fig. 4(*a*), an interfacial energy of 200 erg/cm^2 gives good agreement at 700°C, indicating that this energy must be equal to or less than this value when μ_0 is finite. Using this σ, we now choose μ_0 at each temperature so as to optimize agreement with the experimental data on V as a function of $(C_0 - C_\infty)$. These results are shown in Fig. 5, and the values of μ_0 thus obtained are given in Table IV. With these values of σ and μ_0 fairly good agreement is also obtained with the radius of curvature measurements, as shown in Fig. 6.

Partitioning of Supersaturation

Partitioning of the free energy of transformation into various physical processes can be easily visualized by the use of the free energy-composition diagram shown in Fig. 7. The dotted curve is for the case of a flat interface. We have followed Hillert[22] in assuming that the capillarity effect changes the pressure only in the precipitate, so that the curvature effect shifts upwards just the curve for ferrite. Recall that C_0, C_ρ, and C_t are the compositions of the austenite at the α-γ boundary corresponding to equilibrium with a flat interface, equilibrium with a curved interface and to the nonequilibrium case, respectively. Corresponding changes in

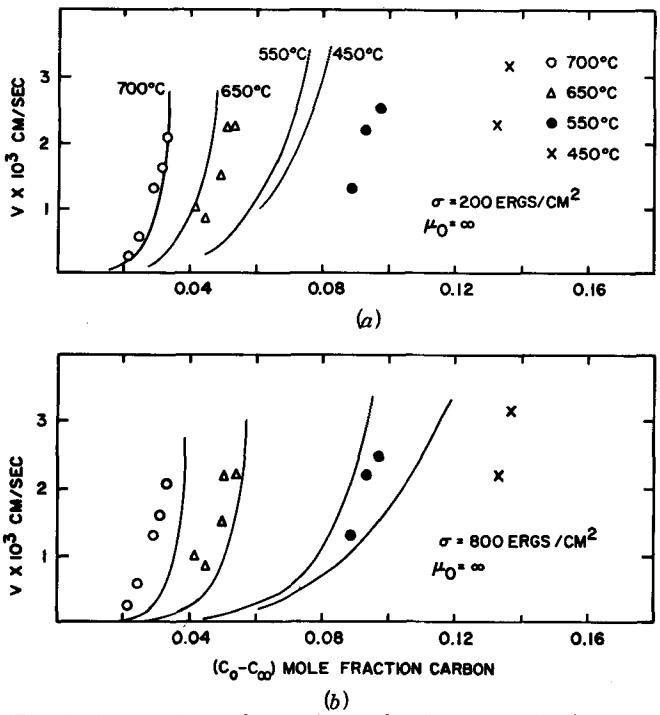

Fig. 4—Comparison of experimental and predicted velocity as a function of driving force for infinite interface kinetics and an assumed surface energy of (*a*) 200 ergs/cm^2 and (*b*) 800 ergs/cm^2.

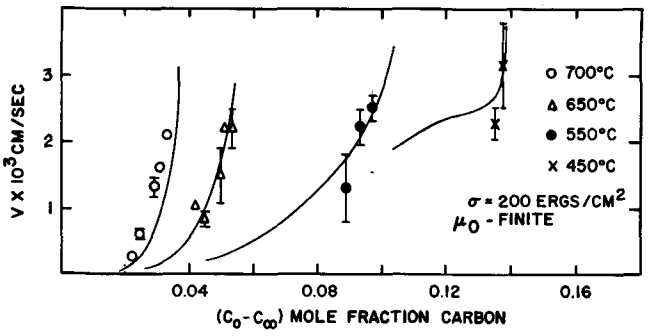

Fig. 5. Comparison of experimental and predicted velocity as a function of driving force for an assumed surface energy of 200 ergs/cm^2 and finite interface kinetics. Error limits represent 50 pct confidence.

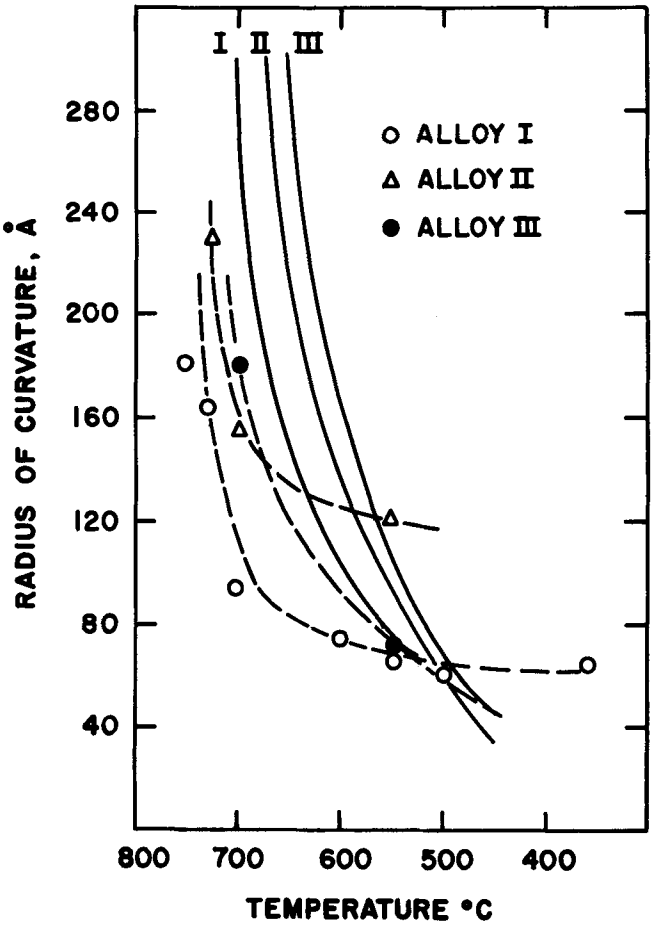

Fig. 6—Experimental and theoretical radii vs. temperature for the indicated alloys.

Table IV. The Predicted Kinetic Parameter as Determined from the Experimental Lengthening Rate at the Indicated Temperatures

	Kinetic Parameter
T, °C	μ_0, cm, Sec-Mole Fraction
700	0.60
650	0.30
550	0.09
450	0.07

precipitate compositions are so small that, for the sake of clarity, only C_p, the equilibrium concentration at a flat interface, is shown in the figure. The free energy changes associated with diffusion, interface motion and capillarity are given by ΔG_d, ΔG_k, and ΔG_c, respectively. From the nature of the present experiments, however, it is simpler to evaluate the relative supersaturations, rather than the relative free energy changes produced by these effects. The two quantities are, of course, closely related.

Eq. [1] shows that the supersaturation is divided into three terms which correspond to fractions of supersaturation consumed by volume diffusion, interface motion and capillarity, respectively. Fig. 8(*a*) plots these contributions at a given temperature, 700°C, as a function of composition. Volume diffusion is seen to use up most of the available supersaturation and to do so even more pronouncedly as the carbon content decreases, or supersaturation increases. Capillarity consumes a noticeable amount at low supersaturations;

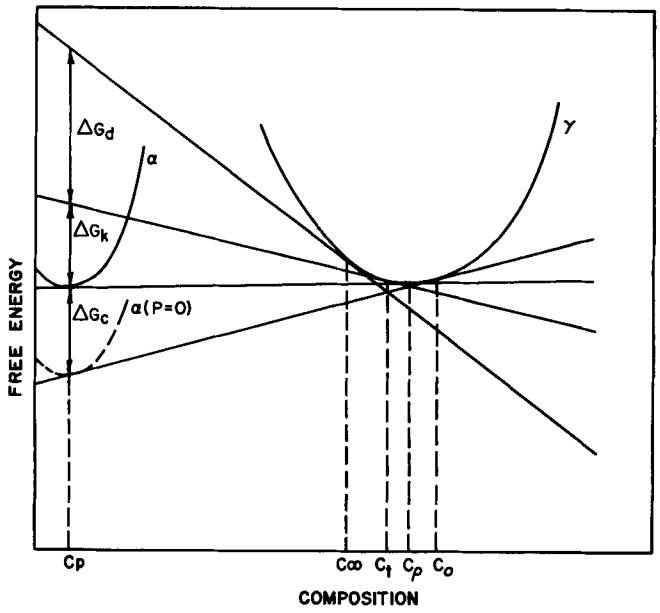

Fig. 7—Schematic free energy-composition diagram for the austenite to ferrite transformation. The ferrite pressure, P, is relative to the pressure in the austenite. ΔG_d, ΔG_k, ΔG_c represent the free energy consumed in solute diffusion, interface kinetics, and capillarity, respectively.

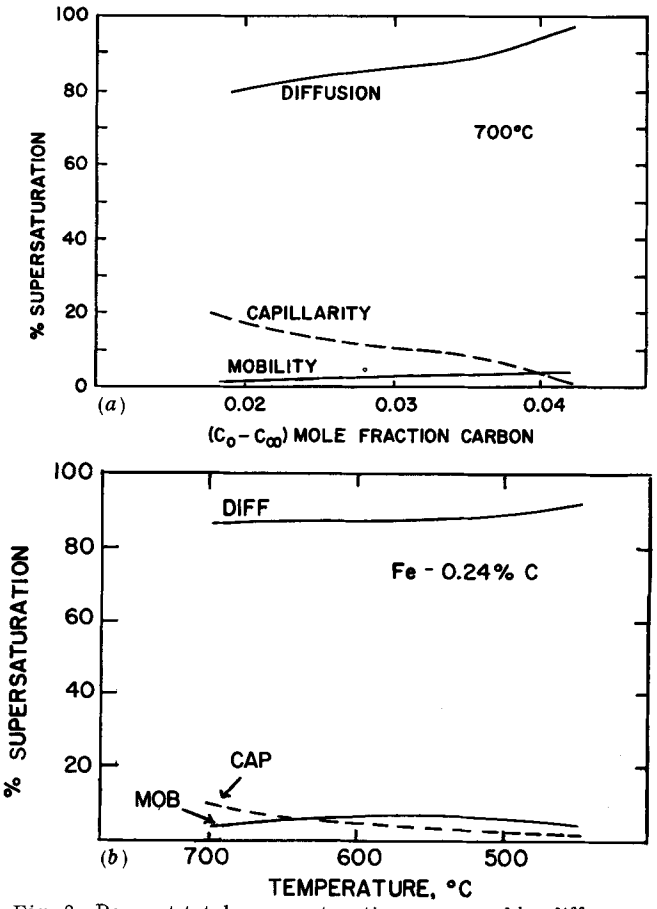

Fig. 8—Percent total supersaturation consumed by diffusion, capillarity, and interface mobility (kinetics) as a function of (*a*) driving force at 700°C and (*b*) temperature in the 0.24 pct C alloy.

at all values studied, the fraction used by interface motion is small, though increasing at higher supersaturations. Similar effects are observed if we consider

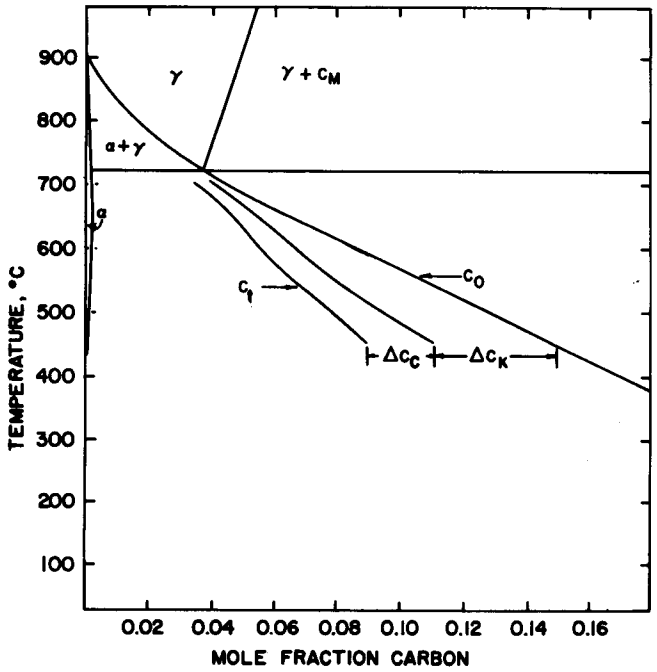

Fig. 9—Fe-C phase diagram where C_0 is given by ADP. The kinetic shift, ΔC_K, and capillary shift, ΔC_C, in the phase boundary are also shown. C_t is the calculated tip concentration.

a fixed composition and study the effects as a function of isothermal reaction temperature, as shown in Fig. 8(*b*). Note that these results are considerably different from the prediction of Zener-Hillert theory,[21,22] which always divides supersaturation equally between volume diffusion and capillarity.

C_t as calculated from the experimental data on Fe-0.24 pct C, is shown in Fig. 9. The decrease in concentration from that for a planar, disordered boundary resulting from capillarity (ΔC_c) and from interface mobility (ΔC_k), can thus be separately assessed as a function of reaction temperature. C_t decreases approximately linearly with increasing temperature in the range shown in Fig. 9:

$$C_t \sim 0.23 - 0.0002T \qquad [6]$$

Structure and Energetics of Ferrite Plate Edges

We shall now consider the values of interfacial energy and mobility in terms of the nature of the edges of ferrite sideplates during the lengthening of Widmanstätten sideplates. The conclusion that σ is of the order of 200 erg/cm^2 is a good indication that the edges of ferrite plates have a ledge structure. This is consistent with the optical and electron microscopic observations of the edges of ferrite plates recounted in the Introduction. The only available calculation of the energy of a dislocation austenite:ferrite boundary yields 200 erg/cm^2, Refs. 30 and 31. This is based, however, upon a martensitic interfacial structure, which the results of Hall *et al.*[8] indicate is unlikely to obtain at the interphase boundaries of ferrite plates. On the other hand, this value can probably be regarded as a reasonable one for an interface composed predominantly of nearly coherent facets with short risers of disordered structure.

Since the rate of lengthening is constant, the spacing between the ledges at a given temperature and composition must be fixed. However, since it is likely that the spacing is physically related to the radius of curvature, which varies with temperature and composition, similar behavior is to be expected of the spacing. This behavior is very different from that of the ledges at the broad faces of ferrite plates, whose spacing is very roughly temperature and composition independent, but exhibits order-of-magnitude scatter under given conditions and also decreases by about an order of magnitude with increasing growth time.[7] However, the mechanism of ledge "nucleation" at the broad faces is evidently of a quite different, and much more random character than that operating at the plate edges.

The theoretical model from which the interfacial energy, and thus structure were derived is phenomenological in nature. It is valid for a ledged boundary as long as the diffusion distance in the matrix is much larger than the spacing between the ledges near the edge of the plate. This condition appears to be fulfilled under the conditions of the present experiments, since the spacing between the ledges near the tip, even for the smallest observed radius of curvature, will be a fraction of this radius. The diffusion distance, on the other hand, is several-fold larger than the radius of curvature. Establishing a direct connection between the theoretical model and the details of the ledge structure (spacing between ledges, height of the risers between them and mobility of the risers), however, does not presently appear to be feasible. Although the growth of isolated ledges along an otherwise flat interface of effectively infinite extent now appears to be well understood,[5,32] the situation at the edge of a ferrite plate is much more complicated. In this case, the ledges are so close together that their diffusion fields doubtlessly overlap; the amount of overlap almost certainly increases the more closely the tip of the plate is approached. That there is no simple connection between μ_0 and the ledge structure is indicated by the failure of the activation energy for the μ_0 values listed in Table IV—11.8 kcal/mole—to correspond to any diffusion process which might be involved in the lengthening of ferrite plates.[33] However, the finding that very little supersaturation is consumed by the finite mobility aspect of plate lengthening, shown in Fig. 8, offers qualitative support for the operation of the ledge mechanism in the customary manner. The risers of ledges, having a disordered structure, should require very little driving force for their displacement.

To conclude in more general fashion, we note that this paper is one of many which have sought to analyze the lengthening rate of ferrite, bainite, and other plates on the basis of a diffusional model.[1,13,14,16-18,21-24,26] Implicit in each of these analyses is the assumption that all areas of the plate edges allow the transfer of iron atoms from austenite to ferrite and the rejection of carbon atoms into the austenite to occur with equal facility—and with the exception of the analysis[17] used in the present paper—to take place without hindrance. It now seems clear that this purely diffusional approach ought not to be further refined. Although the ledge growth problem outlined is a very difficult one, solution of this problem is necessary if further progress is to be achieved in respect to understanding the mechanism and kinetics of the lengthening of ferrite and bainite plates.

SUMMARY

The lengthening rate of ferrite and bainite sideplates and the radius of curvature of the edges of these plates were measured over various ranges of reaction temperature in three high-purity Fe-C alloys, varying in composition from 0.24 pct C to 0.43 pct C. The lengthening rates are generally consistent with those previously obtained for Fe-C alloys by Hillert[14] and by Townsend and Kirkaldy.[18] The radius of curvature data were reported as histograms; the most frequently occurring value was used for analytical purposes. In accordance with the maximum growth rate principle,[20] the width of the histograms decreased with the temperature of transformation.

These data were analyzed on the basis of an equation due to Trivedi.[17] This equation takes separate account of the supersaturation consumed in driving the volume diffusion of solute, in compensating for capillarity and in displacing an interphase boundary of finite mobility. It was found that nearly all of the supersaturation is consumed in the diffusion of carbon in austenite; both capillarity and boundary displacement were found to be relatively minor sources of free energy dissipation under most circumstances. Ascertaining that the lengthening rate data could not be explained with a single reasonable value of the interfacial energy when the interface kinetic coefficient, μ_0, was assumed to be infinite, it was concluded that the sideplate edges are characterized by a finite mobility. The interfacial energy, σ, of these edges is of the order of 200 erg/cm^2. Using this energy, μ_0 was evaluated by fitting the lengthening rate data. These σ and μ_0 data gave fairly good predictions of the variation of the radius of curvature with reaction temperature.

The combination of the low value of σ, the finiteness of μ_0 and the small amount of supersaturation needed to drive the edges of sideplates, taken in conjunction with published observations of ledges on the edges of sideplates[12] and electron microscopy studies on the structure of nearly coherent boundaries between bcc precipitates in an fcc matrix,[8] indicate that ferrite and bainite sideplates lengthen by a ledge mechanism. Since the diffusion distance of the plate edges as a whole must be considerably greater than that of an individual ledge, the continuum model employed by the Trivedi equation is applicable. However, overlapping of the diffusion fields of adjacent ledges prevents a physical interpretation of the μ_0 values in terms of the details of the ledge structure.

REFERENCES

1. H. I. Aaronson: *Decomposition of Austenite by Diffusional Processes,* p. 387, Interscience Publishers, New York, 1962.
2. C. Laird and H. I. Aaronson: *Trans. TMS-AIME,* 1968, vol. 242, p. 1393.
3. H. I. Aaronson and C. Laird: *Trans. TMS-AIME,* 1968, vol. 242, p. 1437.
4. C. Laird and H. I. Aaronson: *Acta Met.,* 1967, vol. 15, p. 73.
5. C. Laird and H. I. Aaronson: *Acta Met.,* 1969, vol. 17, p. 505.
6. K. R. Kinsman, H. I. Aaronson, and E. Eichen: *Met. Trans.,* 1971, vol. 2, p. 1041.
7. K. R. Kinsman, E. Eichen, and H. I. Aaronson: unpublished research, Ford Motor Co., Dearborn, Mich., 1970.
8. M. G. Hall, H. I. Aaronson, and K. R. Kinsman: *Surface Science,* in press.
9. G. R. Purdy: *Mat. Sci. J.,* 1971, vol. 5, p. 81.
10. H. I. Aaronson, C. Laird, and K. R. Kinsman: *Phase Transformations,* p. 313, ASM, Metals Park, Ohio, 1970.
11. E. Eichen, H. I. Aaronson, G. M. Pound, and R. Trivedi: *Acta Met.,* 1966, vol. 14, p. 1637.
12. A. T. Davenport: private communication, Republic Steel Corp., Independence, Ohio, 1971.
13. L. Kaufman, S. V. Radcliffe, and M. Cohen: *Decomposition of Austenite by Diffusional Processes,* p. 313, Interscience Publishers, New York, 1962.
14. M. Hillert: unpublished research, quoted in Ref. 13.
15. G. R. Speich and M. Cohen: *Trans. TMS-AIME,* 1960, vol. 218, p. 1050.
16. H. W. Paxton and G. M. Pound: *Trans. TMS-AIME,* 1963, vol. 227, p. 957.
17. R. Trivedi: *Met. Trans.,* 1970, vol. 1, p. 921.
18. R. D. Townsend and J. S. Kirkaldy: *Trans. ASM,* 1968, vol. 61, p. 605.
19. H. I. Aaronson, N. A. Gjostein, H. W. Paxton, and R. W. Heckel: *Rev. Sci. Inst.,* 1957, vol. 28, p. 579.
20. F. Yost and R. Trivedi: unpublished research, Iowa State University, Ames, Iowa, 1970.
21. C. Zener: *AIME Trans.,* 1946, vol. 167, p. 550.
22. M. Hillert: *Jernkontorets Ann.,* 1957, vol. 141, p. 757.
23. G. P. Ivantsov: *Dokl. Akad. Nauk, SSSR,* 1947, vol. 58, p. 567.
24. R. Trivedi and G. M. Pound: *J. Appl. Phys.,* 1961, vol. 32, p. 2587.
25. C. Wells, W. Batz, and R. F. Mehl: *AIME Trans.,* 1950, vol. 188, p. 553.
26. R. Trivedi and G. M. Pound: *J. Appl. Phys.,* 1967, vol. 38, p. 3569.
27. S. Ban-ya, J. F. Elliott, and J. Chipman: *Met. Trans.,* 1970, vol. 1, p. 1313.
28. H. I. Aaronson, H. A. Domian, and G. M. Pound: *Trans. TMS-AIME,* 1966, vol. 236, p. 753.
29. L. H. Van Vlack: *Trans. TMS-AIME,* 1951, vol. 191, p. 251.
30. H. Knapp and U. Dehlinger: *Acta Met.,* 1956, vol. 4, p. 289.
31. L. Kaufman and M. Cohen: *Prog. Met. Phys.,* 1958, vol. 7, p. 165.
32. G. Jones and R. Trivedi: *J. Appl. Phys.,* 1971, vol. 42, p. 4299.
33. E. P. Simonen: Ph.D. Thesis, Iowa State University, 1972.